Study of Impedance Spectra for Dry and Wet EarEEG Electrodes

Simon L. Kappel[1] and Preben Kidmose[1]

Abstract— **EarEEG is a novel recordings concept where electrodes are embedded on the surface of an earpiece customized to the individual anatomical shape of the users ear. A key parameter for recording EEG signals of good quality is a stable and low impedance electrode-body interface. This study characterizes the impedance for dry and wet EarEEG electrodes in a study of 10 subjects. A custom made and automated setup was used to characterize the impedance spectrum from 0.1 Hz - 2 kHz. The study of dry electrodes showed a mean (standard deviation) low frequency impedance of the canal electrodes of 1.2 MΩ (1.4 MΩ) and the high frequency impedance was 230 kΩ (220 kΩ). For wet electrodes the low frequency impedance was 34 kΩ (37 kΩ) and the high frequency impedance was 5.1 kΩ (4.4 kΩ). The high standard deviation of the impedance for dry electrodes imposes very high requirements for the input impedance of the amplifier in order to achieve an acceptable common-mode rejection. The wet electrode impedance was in line with what is typical for a wet electrode interface.**

I. Introduction

Electroencephalography (EEG) is a non-invasive method for recording signals, that represents aggregated electrical activity from populations of temporally synchronized and spatially aligned neurons, in the brain. EEG recording systems have found widespread use within both clinical practice and in neuroscience. Over the past decades lots of effort has been put into the development of wearable EEG systems, that open new opportunities for monitoring brain activity under less restrictive conditions [1]. The wearable systems aims to be less obtrusive and more user-friendly and thereby enabling brain monitoring in the user's everyday environment. A recent innovation in wearable EEG is the so-called EarEEG in which the EEG is recorded from devices placed in the ear [2][3][4]. The EarEEG device comprises electrodes embedded on an earpiece customized to the individual anatomical shape of the users ear. Due to the limited space on the earpiece, a trade-off between electrode size and electrode distance result in electrode sizes that are smaller than typical surface EEG electrodes.

A key parameter for recording EEG signals of good quality is a stable and low impedance electrode-body interface. Traditionally, this is modeled as an electrochemical electrode-electrolyte interface (EEI). The importance of a low impedance of the EEI is two fold 1) The impedance generates thermal noise as described by the Johnson-Nyquist equation. 2) The current noise of the amplifier is converted to voltage noise through the impedance. Thus, everything else equal, a higher impedance will lead to a higher noise level. EEG signals are measured as differential potentials between two (or more) electrodes, and imbalances in the impedances of these electrodes implies that a common mode signal on the body will be transformed to a differential mode signal on the input of the instrumentation amplifier. As the amplitudes of EarEEG recordings are in the range of a few microvolts and typical common mode noise on the body is in the volts range, the CMRR of the complete instrumentation must be at least 120dB to enable meaningful recordings of EEG [5]. In order to obtain a CMRR of 120dB, the ratio between the input impedance of the instrumentation amplifier and the impedance mismatch between the electrodes must be larger than 6 orders of magnitude [6]. The impedance is highly frequency dependent, and the impedance spectrum must therefore be characterized to enable analysis and modeling of the impedance [7][8]. This paper describes a method to measure and model the electrode impedance spectrum, and presents an empirical study of impedance spectra for dry and wet EarEEG electrodes.

[1]S. L. Kappel and P. Kidmose are with Department of Engineering, Aarhus University, DK-8200 Aarhus N, Denmark.

II. Methods

Impedance is a concept applicable under the assumption of a linear relationship between voltage and current. The impedance of an electrical circuit can, as established by Ohms law, be determined as the ratio between voltage and current. The objective of this work is to characterize the electrode-electrolyte interface (EEI) in terms of the impedance spectrum. However, the EEI is a complex electrochemical system where the Butler-Volmer equation describes how the electrical current through the EEI depends on the overpotential. Above an equilibrium exchange current (EEC) this relationship have highly non-linear behavior, and the impedance measure is thus only applicable below the EEC [9]. Huigen et al. described the EEC to be in the area of a few $\mu A/cm^2$ [10, p12]. An increased current density leads to an increased SNR of the impedance measurements. Thus, the current density used in this study to characterize the impedance spectra, was a tradeoff between a sufficiently high SNR and the need for a current density below EEC.

A. Impedance spectrum characterization

The EarEEG earpieces used for the characterization were 3D printed in hard acrylic plastic and had 6 silver electrodes embedded on the surface as shown to the right in Fig. 1. The electrodes were positioned according to the scheme described by Kidmose et al. [3]; 4 rectangular electrodes (size = 2.8 x 5 mm) on positions E, G, I and K in the ear-canal and 2 circular electrodes (diameter = 6 mm) on positions A and B in the concha part of the outer ear. The positions have been used in previous studies and were found to have a high

978-1-4244-9270-1/15/$31.00 ©2015 IEEE

performance when compared to scalp EEG [4].
Fig. 1 show the schematic of the circuit that was used to characterize the impedance spectrum, $Z(\omega)$, of a dual EEI. R_L is a fixed resistor limiting the current through Z and R_I is a fixed resistor enabling the calculation of the current through $Z(\omega)$ when the voltage over R_I is measured. All the capacitors are parasitic, and will be discussed later.

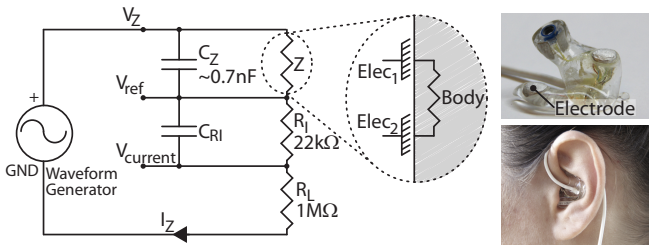

Fig. 1. Schematic of the circuit used to characterize the impedance spectrum of the interface between two electrodes connected to the terminals of Z. The EarEEG device is shown to the right.

An Agilent 33552B waveform generator was used to create an excitation signal containing a mixture of 58 sinusoids that was logarithmically distributed in the range from 0.1 Hz to 2 kHz. The reference input of a g.tec USBamp EEG amplifier was connected to the V_{ref} terminal (Fig. 1) and ch1 and ch2 of the amplifier were connected to V_Z and $V_{Current}$ respectively. The current was then calculated as: $I_Z(\omega) = -V_{Current}(\omega)/R_I$, and the impedance spectrum was calculated according to Ohms law:

$$Z(\omega) = V_Z(\omega)/I_Z(\omega) \quad (1)$$

Measurements of the impedance spectrum for several combinations of electrodes were necessary to enable estimation of the impedance spectrum of a single EEI. To perform the measurements systematically and fast the impedance spectrum measurement setup (ISMS) described above was automated by adding a custom made printed circuit board (PCB) containing a microcontroller and 44 relays. The PCB enabled measurements of the impedance spectrum between all combinations of the 6 electrodes on each earpiece. A Matlab graphical user interface was programmed to control the relays, the waveform generator and the EEG amplifier. With this setup the impedance spectrum from 0.1 Hz to 2 kHz could be estimated for both ears (12 electrodes) in 9 minutes. During testing of the ISMS, measurements indicated parasitic components in the setup. A parasitic capacitance parallel to Z, C_Z, was identified. In order to estimate the value of C_Z, the ISMS was used to characterize the impedance spectra of fixed resistors with a resistance in the range from 10 kΩ to 3.3 MΩ. The value of C_Z was then estimated to 0.7 nF by fitting a parametric model of a resistor parallel to a capacitor to each of the impedance spectra. C_Z was found to be stable across recordings and the effect of C_Z was compensated in the data analysis. Measurements also indicated that a R_I above 100 kΩ introduced effects of parasitic capacitance, C_{RI}, in the recorded impedance spectrum. However, the effect diminished when the value of R_I was reduced to 22 kΩ.

B. The study

An empirical study of dry and wet electrode impedance spectra of 10 subjects (8 males) were conducted. The subjects had their ears cleaned with alcohol prior to the dry electrode measurement, and prior to the wet electrode measurements the ears were also cleaned with abrasive gel and alcohol to remove dead skin cells in the ear-canal and outer ear. For the wet electrode recordings a thin layer of conductive electrode gel (ELEFIX electrode paste) were applied to the surface of each electrode on the earpiece. The impedance spectrum was measured for 8 electrode combinations on each ear. The amplifiers ground plug was connected to an elastic bracelet on the right arm. The bracelet was wet and had silver wires on the inside causing a low and stable impedance to the skin. The impedance spectrum of a dual EEI is dominated by the electrode with the highest impedance. To ensure that a high impedance of a single EarEEG electrode would not dominate the impedance spectrum, 6 recordings were performed with a reference bracelet, similar to the ground bracelet, on left arm as one of the electrodes. The remaining two recordings were performed between electrodes ExK/ExG and ExI/ExE. For the characterization of dry electrodes a mean current density of 200 $\mathrm{nA_{RMS}/cm^2}$ was used and for wet electrodes the mean current density was 1100 $\mathrm{nA_{RMS}/cm^2}$.

C. Parameter fit

To enable quantitative comparison of the impedance spectra across electrodes and subjects, a parametric model of the EEI was introduced. The model is sketched in the upper right corner of Fig. 2 and is a commonly used and simple model of the EEI for a single electrode [11]. R_2 models the ohmic resistance of the electrolyte, and the interface between the electrolyte and electrode is modeled by C_1 and R_1.
Each of the 8 impedance spectra, measured from each ear, represents a double EEI. Therefore, before fitting the parametric model of the EEI to the impedance spectra, it was necessary to estimate the single EEI spectra. The measured impedance spectra can be expressed as a set of linear equations of the single EEI impedance spectra, and the single EEI impedance spectra were estimated using the pseudo inverse of the mixing matrix. This was done for each frequency point, and estimated the single EEI impedance spectra for all 6 electrodes on each earpiece.

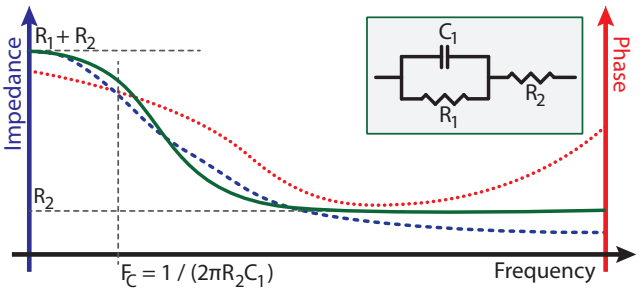

Fig. 2. Sketch of an impedance spectrum measurement. The dashed blue line is the magnitude and the dotted red line the phase of the impedance. The solid green line is a parameter fit of the parametric model sketched in the upper right corner of the figure.

Fig. 2 shows a sketch of a single EEI impedance spectrum, where the dashed blue line is the magnitude and the dotted red line the phase of the impedance. The solid green line illustrates a least square fit between the measurements and the parametric model. More formally, the parameters of the model were collected in a parameter vector:

$$\theta = [R_1, R_2, C_1]^T \tag{2}$$

The cost function was the squared distance between the measured and modeled impedance summed over the frequencies in the excitation signal:

$$J(\theta) = \sum_{n}^{N} |H_{meas}(\omega_n) - H_{model}(\omega_n, \theta)|^2 \tag{3}$$

where $H_{meas}(\omega_n)$ and $H_{model}(\omega_n)$ represents the measured impedance and the modeled impedance spectrum respectively. The parameters were then estimated as:

$$\min_{\text{s.t. } R_1,C_1,R_2>0} J(\theta) \tag{4}$$

Because the frequencies of the sinusoids in the excitation signal were logarithmic distributed the cost function favor low frequencies. The parameter fitting method and the ISMS were validated by connecting component networks with the same structure as the parameter model and known component values.

III. Results

Fig. 3 shows the grand average of the impedance spectra across subjects for (a) dry electrodes in the ear-canal (b) wet electrodes in the ear canal and (c) A and B electrodes in the concha. The dry electrode recordings from the A&B electrodes were left out because the impedance spectra of all subjects showed that the electrodes had no galvanic contact with the skin. The histogram in the upper right corner show the distribution of the mean impedance in the range from 0.1 Hz to 10 Hz. A few recordings, marked by "Rem.", were outliers in the histogram and left out of the analysis. Additionally, 8.7 % of the dry electrode recordings were left out, because C_1 was estimated to an extreme value above 5 µF. In total 6.7 % of the wet and 20 % of the dry electrode data were left out of the analysis.

Table I and II summarizes the results of the parameter fits for dry and wet electrodes respectively.

Based on the parameter values for the canal electrodes of both ears, the mean (standard deviation) low frequency impedance for the dry electrodes was 1.2 MΩ (1.4 MΩ) and the high frequency impedance was 230 kΩ (220 kΩ). For wet electrodes the low frequency impedance was 34 kΩ (37 kΩ) and the high frequency impedance was 5.1 kΩ (4.4 kΩ). The low frequency impedance was estimated as the sum of R_1 and R_2, and the high frequency impedance was estimated as the value of R_2.

Fig. 3, table I and II show that the impedance were one to two orders of magnitude higher for the dry compared to the wet electrodes. Everything else being equal, this will lead to higher thermal and current noise levels. In addition, the standard deviation is also scaled by one to two orders of magnitude. Consequently, in order to achieve the same CMRR on the input of the instrumentation amplifier, the input impedance of the amplifier must also be increased by one to two orders of magnitude [6]. For example, if a CMRR of 120 dB is required, and if the impedance mismatch of an electrode pair is 1 MΩ, the input impedance of the amplifier must be 1 TΩ. This illustrates the trade-offs between CMRR and noise performance that need to be taking into consideration in the design of an appropriate instrumentation amplifier.

From Fig. 3, table I and II it was also observed that the capacitance of the dry electrode interface was much lower

TABLE I

Parametric values for dry electrodes. The left column for the left and right ear is the parameter values from a parametric fit of the grand averaged impedance spectra, whereas the center column is the grand averaged parameter values with the standard deviation, σ, to the right.

		Left ear			**Right ear**			**Both ears**	
		G Avg	Mean	σ	G Avg	Mean	σ	Mean	σ
$\leftarrow R_1[k\Omega]\rightarrow$	ExK	180	190	220	540	620	580	390	470
	ExG	110	110	110	1100	1200	1400	640	1100
	ExE	72	93	78	2100	2500	3400	1200	2500
	ExI	790	860	1600	2500	2800	3300	1800	2700
	Canal	280	270	400	1500	1600	1600	940	1300
$\leftarrow C_1[nF]\rightarrow$	ExK	16	840	1300	12	370	650	620	1000
	ExG	26	420	780	5.2	280	700	350	720
	ExE	190	360	360	6.9	53	91	220	310
	ExI	4.7	770	1700	3.6	81	140	430	1200
	Canal	13	390	590	5.7	240	620	320	590
$\leftarrow R_2[k\Omega]\rightarrow$	ExK	92	90	76	220	210	220	140	170
	ExG	74	73	65	320	290	290	180	230
	ExE	69	55	33	510	370	450	200	340
	ExI	240	180	270	510	370	220	280	260
	Canal	120	110	120	390	350	240	230	220

TABLE II

Parametric values for wet electrodes. The table have the same structure as table I.

		Left ear			**Right ear**			**Both ears**	
		G Avg	Mean	σ	G Avg	Mean	σ	Mean	σ
$\leftarrow R_1[k\Omega]\rightarrow$	ExK	28	29	38	25	28	48	29	42
	ExG	36	39	54	22	23	28	32	43
	ExE	41	46	55	15	15	11	31	43
	ExI	32	35	46	22	26	29	31	39
	ExA	19	19	20	9.6	10	3.5	15	15
	ExB	13	14	15	9.6	10	5.2	12	12
	Canal	34	36	47	21	22	22	29	37
	A&B	16	16	16	9.6	10	4.0	13	12
$\leftarrow C_1[nF]\rightarrow$	ExK	6400	17e3	10e3	6300	15e3	12e3	16e3	11e3
	ExG	5800	14e3	8900	5500	15e3	14e3	14e3	11e3
	ExE	4800	12e3	8100	9700	22e3	20e3	17e3	15e3
	ExI	5300	10e3	5700	6700	12e3	8100	11e3	6700
	ExA	6900	13e3	8100	11e3	13e3	5300	13e3	6700
	ExB	9900	16e3	9100	10e3	16e3	8300	16e3	8500
	Canal	5500	12e3	7100	6800	11e3	8300	12e3	7500
	A&B	8100	14e3	7700	10e3	14e3	6400	14e3	6900
$\leftarrow R_2[k\Omega]\rightarrow$	ExK	5.8	5.7	5.1	5.4	5.5	5.8	5.6	5.3
	ExG	5.4	5.4	5.8	4.2	4.3	5.5	4.9	5.5
	ExE	7.2	7.3	7.6	3.6	3.6	2.3	5.5	5.9
	ExI	5.1	5.2	4.3	3.8	3.9	3.2	4.6	3.8
	ExA	3.6	3.5	2.3	2.4	2.4	1.2	3.0	1.9
	ExB	2.2	2.2	1.3	2.1	2.1	0.92	2.1	1.1
	Canal	5.9	5.9	5.6	4.3	4.2	2.7	5.1	4.4
	A&B	2.9	2.8	1.5	2.2	2.2	0.93	2.5	1.2

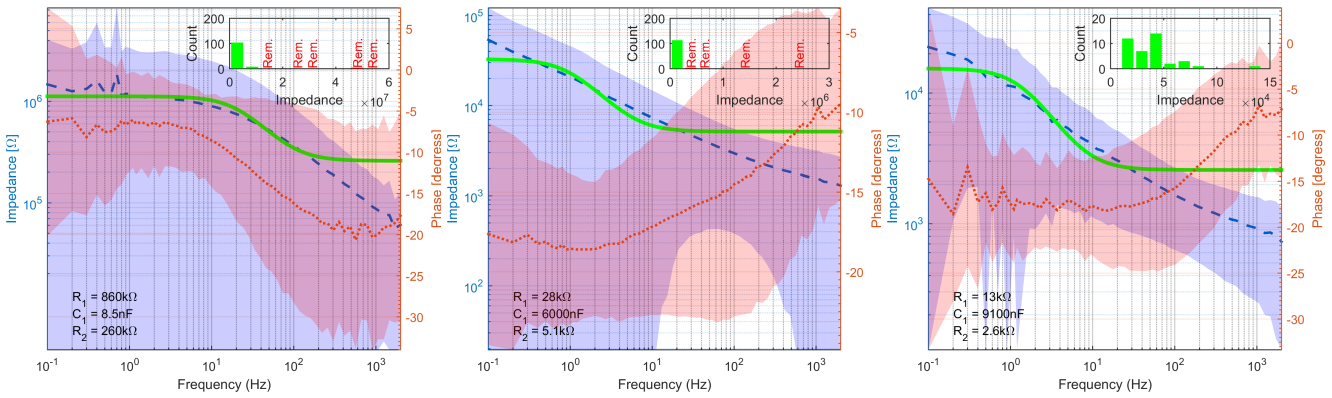

(a) Dry electrodes in ear-canal (b) Wet electrodes in the ear-canal (c) Wet electrodes A and B in concha

Fig. 3. Averages across subjects and electrodes in (a)+(b) the ear-canal and (c) the concha. The dashed blue line is the magnitude and the dotted red line the phase of the impedance. The faded blue and red areas represent the standard deviation of the magnitude and phase respectively. The solid green line is the parameter fit, as described in section II-C, and values given in the lower left corner are the parametric values of the parameter fit. The histogram in the upper right corner depict the distribution of the mean impedance from 0.1 Hz to 10 Hz. The red bars in the histogram marked with "Rem." indicate recordings that were outliers and left out in the analysis.

than the capacitance of the wet interface. It is conjectured that the large difference in electrode capacitance can be explained by how the capacitance is formed: for wet electrodes the capacitance is dominated by the double layer in the EEI, whereas in the dry interface the capacitance, to a larger extent, is formed by the geometrical area between the electrode and the body. However, to the extent that the dry electrode in reality is semi wet, the capacitance will also be influenced by a double layer formed on the surface of the electrode, and thus the electrode capacitance can be increased by a nanostructured surface [8].

The wet electrode impedance was relatively low and the variation in the impedance was not problematic. Previous EarEEG recordings with wet electrodes confirm a satisfying impedance [2][3][4], and the impedance is in line with what was expected for a wet electrode interface [10]. Apart from electrode positions ExA and ExB in the dry-contact measurements, no systematic differences in impedance levels between electrode positions were found; the impedance study did therefore not reveal any preferred electrode positions.

IV. Conclusion

A setup to measure the impedance spectrum from 0.1 Hz to 2 kHz in an automatized, fast and reliably way was constructed, and an empirical study of dry and wet EarEEG electrodes were conducted. The study of dry electrodes showed a mean (standard deviation) low frequency impedance of the canal electrodes of 1.2 MΩ (1.4 MΩ) and the high frequency impedance was 230 kΩ (220 kΩ). For wet electrodes the low frequency impedance was 34 kΩ (37 kΩ) and the high frequency impedance was 5.1 kΩ (4.4 kΩ). A dry electrode impedance with this magnitude is not problematic in regard to designing an EEG amplifier with sufficient noise performance. However, the measurements also showed high variations in the impedance, leading to impedance mismatch between the electrodes, demanding a high input impedance to avoid a significant drop in the common mode rejection ratio of the system. For the wet electrodes the impedance is in line with what is typical for a wet electrode interface. The impedance characterization presented in the paper give valuable information that can be used to improve the EarEEG platform even further.

Acknowledgment

This research was supported by the Danish National Advanced Technology Foundation (j.nr. 110-2013-1).

References

[1] A. J. Casson, D. Yates, D. Smith, J. S. Duncan, and E. Rodriguez-Villegas, "Wearable electroencephalography," *IEEE, Engineering in Medicine and Biology Magazine*, vol. 29, pp. 44–56, 2010.

[2] D. Looney, P. Kidmose, C. Park, M. Ungstrup, M. L. Rank, K. Rosenkranz, and D. P. Mandic, "The in-the-ear recording concept: User-centered and wearable brain monitoring," *IEEE Pulse Magazine*, vol. 3, pp. 32–42, 2012.

[3] P. Kidmose, D. Looney, M. Ungstrup, M. L. Rank, and D. P. Mandic, "A Study of Evoked Potentials From Ear-EEG," *IEEE Trans. Biomedical Engineering*, vol. 60, pp. 2824–30, 2013.

[4] S. L. Kappel, D. Looney, D. P. Mandic, and P. Kidmose, "A method for quantitative assessment of artifacts in EEG, and an empirical study of artifacts," *Int. Conf. of the IEEE Engineering in Medicine and Biology Society (EMBC)*, pp. 1686–1690, 2014.

[5] A. C. Metting van Rijn, A. Peper, and C. A. Grimbergen, "High-quality recording of bioelectric events. Part 1. Interference reduction, theory and practice.," *Medical & biological engineering & computing*, vol. 28, pp. 389–97, 1990.

[6] E. Spinelli and M. Haberman, "Insulating electrodes: a review on biopotential front ends for dielectric skin-electrode interfaces," *Physiological measurement*, vol. 31, pp. 183–98, 2010.

[7] L. A. Geddes and R. Roeder, "Measurement of the direct-current (Faradic) resistance of the electrode-electrolyte interface for commonly used electrode materials," *Annals of biomedical engineering*, vol. 29, pp. 181–6, 2001.

[8] P. Pedrosa, E. Alves, N. P. Barradas, P. Fiedler, J. Haueisen, F. Vaz, and C. Fonseca, "TiNx coated polycarbonate for bio-electrode applications," *Corrosion Science*, vol. 56, pp. 49–57, 2012.

[9] W. Franks, I. Schenker, P. Schmutz, and A. Hierlemann, "Impedance characterization and modeling of electrodes for biomedical applications," *IEEE transactions on bio-medical engineering*, vol. 52, pp. 1295–302, 2005.

[10] E. Huigen, "Noise characteristics of surface electrodes," M.S. thesis, University of Amsterdam, Section Medical Physics, 2001.

[11] Y. M. Chi, T. Jung, and G. Cauwenberghs, "Dry-contact and non-contact biopotential electrodes: Methodological review," *Biomedical Engineering, IEEE Reviews in*, vol. 3, pp. 106–119, 2010.